A&A 404, 223–232 (2003)
DOI: 10.1051/0004-6361:20030486

Astronomy & Astrophysics

New infrared star clusters in the Northern and Equatorial Milky Way with 2MASS

E. Bica[1], C. M. Dutra[2], J. Soares[1], and B. Barbuy[2]

[1] Universidade Federal do Rio Grande do Sul, Instituto de Física, CP 15051, Porto Alegre, RS 91501-970, Brazil
[2] Universidade de São Paulo, Instituto de Astronomia, Geofísica e Ciências Atmosféricas, Rua do Matão 1226, Cid. Universitária, São Paulo, SP 05508-900, Brazil

Received 21 January 2003 / Accepted 25 March 2003

Abstract. We carried out a survey of infrared star clusters and stellar groups on the 2MASS J, H and K_s all-sky release Atlas in the Northern and Equatorial Milky Way ($350° < \ell < 360°$, $0° < \ell < 230°$). The search in this zone complements that in the Southern Milky Way (Dutra et al. 2003a). The method concentrates efforts on the directions of known optical and radio nebulae. The present study provides 167 new infrared clusters, stellar groups and candidates. Combining the two studies for the whole Milky Way, 346 infrared clusters, stellar groups and candidates were discovered, whereas 315 objects were previously known. They constitute an important new sample for future detailed studies.

Key words. Galaxy: open clusters and associations: general – infrared: general

1. Introduction

Embedded star clusters allow one to study the very initial phases of star formation. Since they are in general deeply embedded in dust and/or located in heavily reddened lines of sight, the infrared domain is necessary to study them (e.g. Lada & Lada 1991; Hodapp 1994; Deharveng et al. 1997; Carpenter 2000).

A large sample of embedded clusters and the knowledge of their distribution throughout the Galaxy – both angularly and in depth – are fundamental to be established, which in turn is important for subsequent detailed studies of individual objects and of the Galactic structures to which they belong. Besides serendipitous discoveries and findings in specific directions such as those of molecular clouds (Hodapp 1994) or nebulae (Dutra et al. 2003a, hereafter Paper I), systematic methods can be applied: visual inspections of a whole area (Dutra & Bica 2000a) or automated methods (Reylé & Robin 2002; Ivanov et al. 2002).

The near-infrared Two Micron All Sky Survey (hereafter 2MASS, Skrutskie et al. 1997) has become a fundamental tool for the discovery of star clusters and stellar groups in the Galaxy, most of them embedded in dust. A literature compilation of 276 infrared clusters and stellar groups (Bica et al. 2003) included objects reported until mid 2002. Several entries in that catalogue had been found on the basis of 2MASS material. In addition to those objects, Dutra & Bica (2000a) surveyed 2MASS images of central parts of the Galaxy and reported 58 small angular size cluster candidates resembling the Arches and Quintuplet clusters as seen on 2MASS images. Recently, Dutra et al. (2003b) have observed most of them deeper and at higher angular resolution with the ESO NTT telescope: 31 turned out to be blended star images in the 2MASS Atlas, while 27 were confirmed as clusters or remain as cluster candidates.

More recent discoveries are 10 objects from Le Duigou & Knödlseder (2002) and Ivanov et al. (2002) using 2MASS, 2 objects from Deharveng et al. (2002) using their own observations, and finally, 179 objects from Paper I using J, H and K_s images from the 2MASS all-sky release Atlas. In Paper I we performed a search for clusters and stellar groups in the directions of known optical and radio nebulae throughout the Southern Milky Way ($230° < \ell < 350°$).

The present study aims to complete the search for infrared stellar clusters and stellar groups around the Milky Way disk in the directions of known optical and radio nebulae, which was initiated in Paper I. In Sect. 2 we present the search method. In Sect. 3 we provide the newly found objects related to optical and radio nebulae. In Sect. 4 we discuss some properties of the new samples. Finally, in Sect. 5 concluding remarks are given.

2. Search method

Using the same procedures as in Paper I, we searched for infrared clusters and stellar groups in the J, H and K_s 2MASS images around the central positions of optical and radio nebulae in the Milky Way region $350° < \ell < 360°$, $0° < \ell < 230°$. We extracted J, H and K_s images with $5' \times 5'$ centred

Send offprint requests to: C. M. Dutra,
e-mail: dutra@astro.iag.usp.br

on the coordinates of each nebula from the 2MASS Survey Visualization & Image Server facility in the web interface http://irsa.ipac.caltech.edu/. For the nebulae with sizes larger than $5' \times 5'$ we took additional images with size $10' \times 10'$ or $15' \times 15'$. The K_s band images allow one to probe deeper in more absorbed regions, whereas the J and H band images were used to detect blended images by bright star contamination.

The optical nebula list was compiled from: Ber (Bernes 1977), BFS (Blitz et al. 1982), BRC (Sugitani et al. 1991), Ced (Cederblad 1946), DG (von Dorschner & Gurtler 1963), GGD (Gyulbudaghian et al. 1978), GM1- (Gyulbudaghian & Maghakian 1977a), GM2- (Gyulbudaghian & Maghakian 1977b), GM3- (Gyulbudaghian & Maghakian 1977c), Gy1- (Gyulbudaghian 1982a), Gy2- (Gyulbudaghian 1984a), Gy3- (Gyulbudaghian 1984b), Gy82- (Gyulbudaghian 1982b), NS (Neckel & Staude 1984), Parsamian (Parsamian 1965), PP (Parsamian & Petrosian 1979), RNO (Cohen 1980), Sh1- (Sharpless 1953), Sh2- (Sharpless 1959) and vdB-RN (van de Bergh 1966).

Several southern catalogues have extensions to equatorial zones, and have also been investigated: ESO (Lauberts 1982), Gum (Gum 1955), RCW (Rodgers et al. 1960) and vdBH-RN (van den Bergh & Herbst 1975).

The radio nebula list was compiled from: G – Reifenstad III et al. (1970), Downes et al. (1980), Lockman (1989) and Kuchar & Clark (1997), CTB – Wilson & Bolton (1960) and Wilson (1963), and W – Westerhout (1958). We also indicate some infrared nebulae related to sources in the AFGL and IRAS catalogues. The list of SNRs is from Green (2001). The identification of optical SNRs is according to van den Bergh (1978).

Each detection before becoming a discovery was checked against the known objects, i.e. the infrared catalogue (Bica et al. 2003) and optical open cluster catalogues (Alter et al. 1970; Lyngå 1987; Dias et al. 2002) in the studied region.

For the resulting IR star clusters we determined accurate positions and dimensions from their K_s images (in FITS format) using SAOIMAGE 1.27.2 developed by Doug Mink.

3. Newly found objects

Embedded clusters are expected to occur in the areas of nebulae, thus we concentrated our search efforts on known optical and radio nebulae, mostly HII regions but also reflection nebulae and supernova remnants.

We merged the different catalogues and lists of nebulae into a radio/infrared and an optical nebula files. We cross-identified nebulae in each file, and between both files. Radio nebulae with optical counterparts were transferred to the optical nebula file. The resulting input lists of optical and radio nebulae make in total respectively 1361 and 826 objects in the present Milky Way regions, whose directions were inspected. The whole Milky Way radio and optical nebula catalogue currently has 4450 entries after cross-identifications, and will be provided in a forthcoming study. The optical and radio nebula catalogues are similar to the recent dark nebula catalogue with 5004 entries by Dutra & Bica (2002).

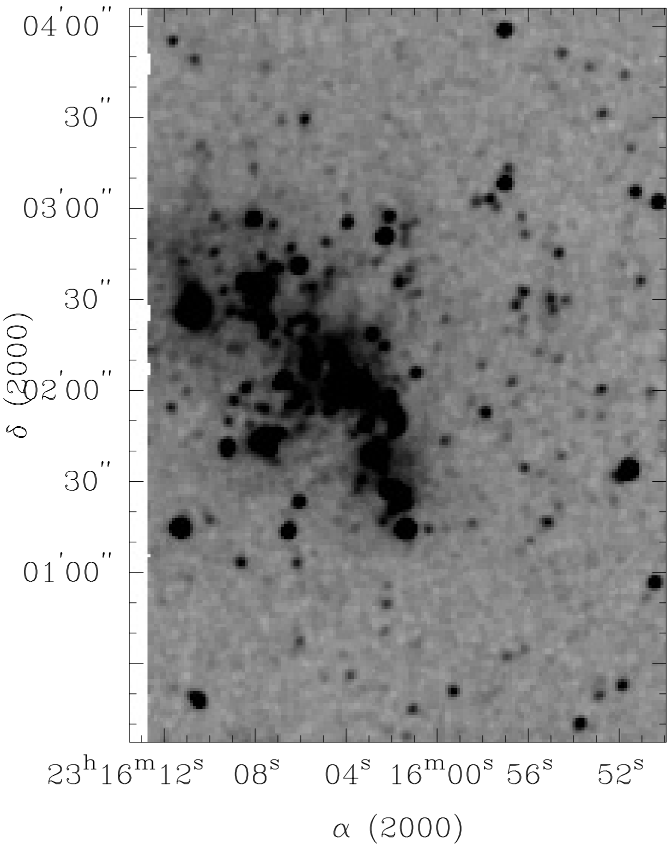

Fig. 1. $4' \times 3'$ 2MASS K_s image of Object 43 in Sh2-157.

The results of the cluster survey are shown in Tables 1 and 2, respectively for optical and radio nebulae. By Cols. (1) running number, (2) and (3) Galactic coordinates, (4) and (5) J2000.0 equatorial coordinates, (6) and (7) major and minor angular dimensions, (8) related nebulae, (9) class, (10) remarks including distance (in case of kinematical ambiguity the near and far distances are shown), multiplicity and linear dimension.

The new infrared clusters, stellar groups and candidates from the optical nebula survey amount to 103, and from the radio nebulae survey they are 64. The detection rates relative to the input nebula catalogues are both 8% for optical and radio nebulae. These detection rates are lower than those obtained in Paper I, mostly because the Equatorial and Northern Milky Way had been previously more surveyed for infrared clusters than their southern counterpart (Paper I). Several reasons may contribute to these low rates: (i) cluster outside the search box owing to projection effects between molecular cloud and champagne flow; (ii) extreme absorption in molecular cloud or in the line-of sight; (iii) HII region ionized by isolated star or stars; (iv) reflection nebula illuminated by single star.

We illustrate in Fig. 1 a prominent infrared cluster in an optical nebula: Object 43 in Sh2-157. We show in Fig. 2 a 14 K_s image of Lagoon's Nebula Hourglass (Woodward et al. 1990). With the 2MASS's resolution an embedded cluster starts to show up. The western part of the Hourglass is particularly resolved into stars. We illustrate in Fig. 3 a prominent infrared cluster located in a radio nebula: Object 165 in

Table 1. New objects in the area of optical nebulae.

Object	ℓ	b	J2000 RA	J2000 Dec	$D(')$	$d(')$	Related Nebulae	Type	Remarks
1	5.97	−1.18	18 03 41	−24 22 40	1.9	1.6	in Lagoon Neb.=M8 = NGC 6523 = W29 = CTB46[a]	IRC	R = 1.0 LD = 0.6
2	6.90	−2.29	18 09 57	−24 06 33	1.9	1.9	in NGC 6559=ESO521*N40, in Sh2-29	IRC	R = 1.4 LD = 0.8 loose
3	8.66	−0.34	18 06 15	−21 37 27	1.1	1.0	in Gum77b=RCW151	IRCC	R = 1.9 LD = 0.6
4	11.48	−1.65	18 16 58	−19 46 58	2.0	1.8	in NGC 6589, in Sh1-36=vdB-RN118 = ESO590N14	IRGr	R = 1.3 LD = 0.8
5	11.42	−1.72	18 17 06	−19 52 10	1.6	1.2	near IC1283, in RCW153	IRGr	
6	12.43	−1.11	18 16 51	−18 41 52	0.9	0.7	in Sh2-39	IRCC	
7	12.64	0.61	18 10 55	−17 41 25	1.9	1.7	in vdB-RN116	IRGr	R = 0.6 LD = 0.3
8	18.14	−0.28	18 25 01	−13 15 47	1.8	1.8	in G18.143-0.289	IRC	R = 4.5 LD = 2.4 deeply emb., lane
9	18.67	1.97	18 17 53	−11 44 26	2.8	2.3	in Gum85 = G18.7+2.0	IRC	R = 2.6 LD = 2.1 Opt/IR loose
10	28.97	−0.60	18 46 21	−3 47 42	1.9	1.3	in G28.983-0.603	IRGr	
11	39.89	−1.27	19 08 43	5 36 02	1.4	1.4	rel RNO108, in Sh2-74 = RCW182=G39.904-1.331	IRGr	
12	53.62	0.04	19 30 23	18 20 46	1.2	1.2	in DG159 = Ber17, in Sh2-82 = AFGL4249	IRGr	R = 1.1 LD = 0.4
13	55.11	2.42	19 24 30	20 47 30	1.3	1.1	in Sh2-83 = G55.114+2.422	IRGr	Opt/IR
14	62.57	2.39	19 40 22	27 18 29	1.0	1.0	in NGC 6813 = IRAS 19383+2711, in W54	IRC	
15	63.15	0.44	19 49 15	26 49 58	1.9	1.8	in Sh2-90 = G63.2+0.4	IRGr	R = 2.0 LD = 1.1
16	64.14	−0.47	19 55 00	27 12 57	1.9	1.7	in Sh2-93 = G64.140-0.470	IRC	R = 2.0 LD = 1.1
17	68.14	0.92	19 59 08	31 21 38	1.7	1.5	in Sh2-98 = G68.134+0.917	IRGr	
18	69.92	1.52	20 01 10	33 11 09	1.2	1.2	in W58G = G69.9+1.5 = G69.942+1.517	IRC	R = 12.4 LD = 4.3
19[b]	77.69	-8.48	21 01 46	33 32 34	0.6	0.5	in K3-50 = W58A = K3-50A	IRCC	R = 8.7 LD = 1.5 not PN
20	80.03	2.69	20 24 21	42 15 56	1.3	1.2	in NGC 6914a = DG162 = vdB-RN131=Ber23, in Sh2-109	IRGr	R = 1.1 LD = 0.4
21	90.23	1.72	21 05 16	49 39 35	1.8	1.8	in Sh2-121 = G90.2+1.7	IRGr	
22	95.67	0.24	21 36 25	52 28 04	1.7	1.3	in BFS6 = G95.7+0.2	IRGr	
23	96.03	4.03	21 20 24	55 28 01	2.2	1.9	in BFS7	IRGr	Opt/IR
24	96.29	2.59	21 28 43	54 37 03	1.9	1.1	in Sh2-127 = G96.3+2.6	IRGr	
25	97.40	8.51	21 02 49	59 30 42	1.7	1.5	in DG168 = BFS9 = GM1-54=RNO130	IRGr	
26	97.51	3.17	21 32 10	55 52 45	1.2	1.2	in Sh2-128 = G97.6+3.2	IRCC	mP,not PN
27	97.53	3.18	21 32 11	55 53 42	0.7	0.7	in Sh2-128 = G97.6+3.2	IRCC	mP,not PN
28	97.95	1.49	21 42 24	54 55 03	0.8	0.8	related to GM1-12 = PP101	IRCC	mP
29	97.97	1.49	21 42 28	54 56 00	1.1	0.8	related to GM1-12 = PP101	IRC	mP
30	105.30	4.05	22 14 41	61 26 04	2.1	2.1	in DG180	IRC	loose
31	105.31	9.93	21 42 00	66 05 12	1.9	1.8	in GM1-57 = PP102 = NS20,rel NGC 7129	IRGr	
32	105.73	4.10	22 17 24	61 43 05	2.3	1.9	in RNO140	IRGr	
33	107.16	−0.97	22 47 48	58 03 55	1.7	1.5	related to GM2-42, in Sh2-142	IRGr	R = 3.4 LD = 1.7
34	108.16	0.60	22 49 10	59 54 54	1.2	1.2	in Sh2-146 = G108.197+0.579	IRC	R = 4.6 LD = 1.6 deeply emb., lane
35	108.36	−1.06	22 56 17	58 31 14	1.7	1.6	in Sh2-148	IRC	R = 5.5 LD = 2.7 deeply emb.
36	108.76	−0.95	22 58 41	58 46 57	2.4	1.8	in Sh2-152 = G108.760-0.952	IRC	R = 3.8 LD = 2.7 deeply emb.
37	109.10	−0.34	22 59 06	59 28 33	1.2	1.0	related to Gy82-13	IRC	deeply embedded
38	109.99	−0.09	23 04 45	60 04 36	1.1	1.1	in BFS15	IRC	R = 6.1 LD = 2.0
39	110.11	0.05	23 05 11	60 14 44	2.0	1.5	in IC1470	IRCC	R = 6.1 LD = 3.5 deeply emb.
40	110.20	2.65	22 56 55	62 39 32	2.9	1.9	in Sh2-155 = CTB108	IRGr	R = 0.7 LD = 0.6 mP
41	110.21	2.62	22 57 05	62 38 16	1.9	1.9	in Sh2-155 = CTB108	IRC	R = 0.7 LD = 0.4 mP loose
42	110.25	0.01	23 06 22	60 16 11	1.7	1.5	related to BFS18, in Sh2-156 = G110.106+0.044	IRC	R = 6.1 LD = 3.0 loose
43	111.29	−0.66	23 16 06	60 02 05	2.2	2.0	in Sh2-157	IRC	R = 2.5 LD = 1.6
44	112.22	0.22	23 20 41	61 11 35	1.1	0.7	in NGC 7635 = Sh2-162 = G112.237+0.226	IRGr	R = 3.5 LD = 1.1 compact,emb.
45	113.58	−0.62	23 33 34	60 50 07	2.4	2.1	in Sh2-163 = G113.589-0.721	IRC	R = 2.3 LD = 1.6 loose
46	114.60	0.22	23 39 44	61 55 45	2.7	2.1	in Sh2-165	IRGr	R = 1.6 LD = 1.3 Opt/IR
47	115.78	−1.58	23 52 58	60 28 30	2.2	1.8	in Sh2-168 = G115.784-1.573	IRC	R = 3.8 LD = 2.4 loose
48	118.62	−1.32	0 15 29	61 15 01	2.8	2.4	in Sh2-172	IRC	loose
49	123.81	−1.78	0 58 40	61 04 45	1.4	1.4	in Ced4a = IRAS 00556+6046	IRGr	
50	124.87	−3.14	1 06 45	59 40 36	2.3	1.7	related to RNO4	IRC	loose
51	124.90	0.32	1 08 50	63 07 40	1.3	1.3	in Sh2-186	IRCC	
52	126.66	−0.79	1 23 06	61 51 23	2.6	1.8	in Sh2-187 = Ber49	IRC	Opt/IR
53	130.10	11.12	2 28 18	72 37 48	1.3	1.3	in RNO7	IRC	loose
54[c]	133.70	1.17	2 25 27	62 03 33	1.1	0.8	in NGC 896, in W3	IRC	R = 2.3 LD = 0.7 m4
55[c]	133.69	1.22	2 25 32	62 06 48	1.2	0.8	in W3	IRC	R = 2.3 LD = 0.8 m4 deeply emb.
56[c]	133.71	1.21	2 25 35	62 05 36	1.9	1.3	in W3	IRC	R = 2.3 LD = 1.3 m4 loose
57	136.12	2.08	2 47 26	61 56 53	1.3	1.1	in Sh2-192	IRCC	
58	137.76	1.50	2 57 28	60 41 37	2.4	2.1	related to LW Cas Nebula=RNO11=PP7[d]	IRGr	
59	143.82	−1.57	3 24 53	54 57 25	1.8	1.4	in BFS31	IRGr	
60	149.08	−1.99	3 51 34	51 29 55	2.7	1.9	related to BFS32=PK149-1.1	IROC	not PN
61	150.59	−0.94	4 03 17	51 19 35	3.2	2.2	in NGC 1491 = G150.590-0.950 = AFGL5111[e]	IRGr	R = 3.3 LD = 3.1
62	150.86	−1.12	4 03 50	51 00 55	1.3	1.3	in Sh2-206 = CTB12	IRCC	R = 3.3 LD = 1.2
63	150.98	−0.47	4 07 12	51 24 53	1.2	1.2	in BFS34	IRCC	
64	151.29	1.97	4 19 33	52 58 42	1.2	1.2	in Sh2-208	IRC	loose
65	151.61	−0.23	4 11 10	51 09 58	2.8	2.0	in Sh2-209 = G151.594-0.228	IRC	R = 4.9 LD = 4.0
66	154.65	2.44	4 36 50	50 52 46	1.6	1.4	in Sh2-211 = G154.640+2.436	IRC	
67	155.36	2.61	4 40 39	50 27 39	2.9	2.0	in Ced37 = IRAS 04366+5022	IRC	loose
68	169.65	−0.07	5 18 11	37 33 31	1.4	1.4	in IC2120 = PK169-0.1	IRGr	not PN
69	173.38	−0.18	5 28 11	34 25 28	3.1	2.8	in IC417 = Sh2-234	IROC	R = 2.6 LD = 2.3 Opt/IR loose
70	173.58	−1.66	5 22 47	33 25 26	2.7	2.3	in Ced43 = IRAS 05189+3327	IRC	loose

Notes: [a] in Hourglass Nebula (Woodward et al. 1990), in Ced152a = IRAS 18009-2427 = G5.956-1.265, [b] triplet with the NGC 6857 and K3-50B clusters (Bica et al. 2003), [c] the present Objects 54, 55 and 56 form a quadruplet with the W3-IRS5 Cluster (Bica et al. 2003), [d] = Gy82-2 = IRAS 02534+6029, [e] in Sh2-206, [f] the present Objects 71, 72 and 73 together with the Sh2-235B Cluster form a quadruplet, [g] in Ced61 = DG86,[h] in Object NGC 6334V (Bica et al. 2003), [i] in NGC 6334=RCW127 = CTB39.

Table 1. continued.

Object	ℓ	b	J2000 RA	J2000 Dec	$D(')$	$d(')$	Related Nebulae	Type	Remarks
71[f]	173.76	2.66	5 40 51	35 38 20	0.8	0.8	in GGD5 = BFS47 = GM2-5 = RNO52S, in Sh2-235B	IRCC	R = 1.8 LD = 0.4 m4
72[f]	173.74	2.69	5 40 54	35 40 22	2.2	2.0	in Sh2-235B	IRC	R = 1.8 LD = 1.2 m4 loose
73[f]	173.69	2.72	5 40 55	35 44 08	0.9	0.9	in GGD6 = GM2-6 = RNO52N, in Sh2-235B	IRCC	R = 1.8 LD = 0.5 m4 loose
74	177.73	–0.34	5 38 47	30 41 18	1.5	1.2	in GM1-40 = PP36	IRGr	deeply embedded
75	180.71	4.33	6 04 30	30 30 07	3.9	2.6	related to vdB-RN65 = PP52 = IRAS 06013+3030[g]	IROC	R = 1.2 LD = 1.4
76	184.00	1.83	6 01 55	26 24 58	1.1	1.1	in GM1-6 = BFS49	IRC	
77	184.87	–1.73	5 50 14	23 52 19	1.3	1.3	in IC2144 = BFS50	IRCC	deeply embedded
78	192.99	0.14	6 14 23	17 44 37	0.9	0.9	in NGC 2195	IRC	
79	193.01	0.13	6 14 23	17 43 12	0.9	0.7	related to in GM1-45	IRGr	mP
80	192.99	0.15	6 14 24	17 44 42	1.4	1.0	related to in GM1-45	IRC	mP
81	196.21	–1.20	6 15 53	14 16 08	2.0	1.7	in Sh2-267 = PK196-1.1	IRC	R = 3.5 LD = 2.0 not PN
82	197.79	–2.31	6 14 57	12 21 03	2.2	1.9	in Sh2-271 = PK197-2.1	IRC	R = 3.3 LD = 2.1 not PN,loose
83	210.34	19.14	5 38 24	–6 24 05	3.0	2.1	in IC428 = Ber120, in LDN1641	IRGr	R = 0.5 LD = 0.4
84	210.79	–2.55	6 38 28	0 44 41	1.5	1.1	in Sh2-283	IRGr	
85	213.84	0.62	6 55 17	–0 31 26	0.8	0.8	in Sh2-285	IRGr	R = 6.9 LD = 1.6
86	215.61	15.03	6 02 16	–9 06 47	0.8	0.6	in GGD10 = GM2-10	IRGr	
87	216.32	15.02	6 03 30	–9 43 50	2.7	2.7	in NGC 2149 = vdB-RN66 = PP51 = RNO61	IROC	R = 0.8 LD = 0.6
88	217.33	–1.36	6 54 36	–4 32 04	2.6	2.0	in Sh2-286	IRGr	
89	217.63	–0.18	6 59 24	–4 15 54	2.5	2.0	in BFS59	IRGr	R = 1.4 LD = 1.0
90	218.20	–0.39	6 59 41	–4 51 44	1.8	1.5	related to Gy3-4 = RNO81, in Sh2-287S	IRC	R = 3.2 LD = 1.7 loose
91	219.47	10.56	6 25 16	–10 33 12	3.6	2.3	related to RNO71	IROC	
92	219.09	–1.54	6 57 11	–6 11 04	3.5	2.9	related to Parsamian 16 = RNO77	IROC	
93	221.01	–2.51	6 57 15	–8 19 48	1.1	1.1	in RNO78	IRC	
94	221.96	–1.99	7 00 51	–8 56 33	1.8	1.6	in RNO82	IRC	loose
95	224.17	1.22	7 16 33	–9 25 20	2.1	1.8	in Sh2-294 = RCW3	IRC	R = 4.6 LD = 2.8 loose
96	225.48	–2.57	7 05 18	–12 19 44	2.7	1.8	in Ced90 = Gum3 = Sh2-297 = RCW1a = vdB-RN94 = Ber134	IROC	R = 1.1 LD = 0.9
97[h]	351.17	0.68	17 20 03	–35 58 18	1.2	1.2	rel. to vdBH-RN85b, in NGC 6334 = RCW127 = CTB39	IRGr	R = 1.6 LD = 0.6 mP
98[h]	351.20	0.70	17 20 03	–35 55 58	0.9	0.7	rel. to vdBH-RN85b, in NGC 6334 = RCW127 = CTB39	IRC	R = 1.6 LD = 0.4 mP
99	351.27	1.01	17 18 59	–35 41 48	1.7	1.3	rel. to vdBH-RN85a, in Gum63[i]	IRGr	R = 1.6 LD = 0.8
100	353.10	0.64	17 25 33	–34 24 03	2.0	1.2	in RCW131b = G353.1+0.7, in Sh2-11 = RCW131 = W22	IRC	R = 1.7 LD = 1.0 mP loose
101	353.11	0.65	17 25 34	–34 23 08	0.8	0.8	in RCW131b = G353.1+0.7, in Sh2-11 = RCW131 = W22	IRC	R = 1.7 LD = 0.4 mP loose
102	355.46	0.38	17 32 52	–32 34 33	1.8	1.3	in Gum67 = Sh2-12 = W23 = RCW132	IRGr	R = 1.4 LD = 0.7
103	358.57	–2.16	17 50 47	–31 16 34	1.7	1.7	in RCW134 = W25	IRC	R = 1.9 LD = 0.9

G351.694-1.165. In Fig. 4 we show Object 139 in the radio nebula W51B = G49.0-0.3, part of the large star-forming complex W51.

Object classes are infrared cluster (IRC), stellar group (IRGr), cluster candidate (IRCC), and open cluster (IROC). Images illustrating these different classes were given in Paper I. IRCs are in general populous and at least partially resolved. IRCCs are probably clusters, but are essentially unresolved, and require higher resolution and deeper images for a definitive diagnostic. IRGrs are less dense than IRCs (Bica et al. 2003), some are rather compact but little populated. IROCs have similar appearence to optical open clusters and relatively large angular size (≈2′ or more). In Table 1 there occur 45 IRC, 37 IRGr, 14 IRCC and 7 IROC objects, while in Table 2 16 IRC, 18 IRGr and 30 IRCC objects. The large fraction of cluster candidates among radio nebulae certainly reflects higher absorption and/or larger distance effects.

Distances are mostly based on kinematical estimates for the nebulae (Downes et al. 1980), but include as well averages with estimates from individual stars, when available (e.g. Georgelin et al. 1973). The near/far distance (R) ambiguity has been solved by Downes et al. (1980) for several nebulae, else we indicate both R_n and R_f. The provided distances in Tables 1 and 2 should be compared to those from the infrared stellar content in future studies.

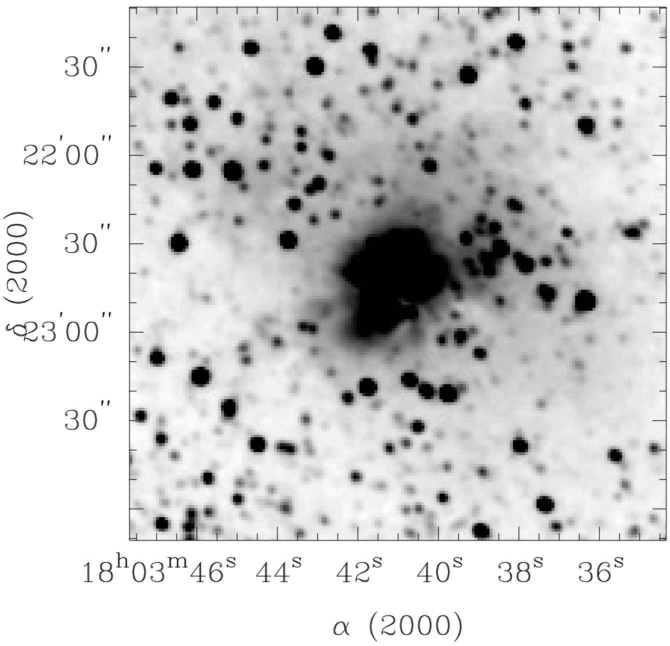

Fig. 2. 3′ × 3′ 2MASS K_s image of Object 1 in Lagoon Nebula´s Hourglass.

Some infrared clusters, stellar groups and candidates were found to be related to nebulae which have been classified

Table 2. New objects in the area of radio/infrared nebulae.

Object	ℓ	b	J2000 RA	J2000 Dec	$D(')$	$d(')$	Related Nebulae	Type	Remarks
104	3.64	−0.10	17 54 25	−25 51 36	1.1	0.9	in G3.662-0.113	IRGr	R_n = 1.5 R_f = 18.5
105	5.20	−2.60	18 07 30	−25 44 30	1.3	1.0	related to radio SNR G5.2-2.6?	IRGr	
106	5.34	−0.99	18 01 35	−24 50 06	1.6	1.4	related to radio SNR G5.321-0.974?	IRGr	
107	5.90	−0.43	18 00 42	−24 04 23	1.2	0.8	in W28A2=G5.9-0.4=G5.899-0.427, in W28=RCW145	IRC	R = 3.0 LD = 1.0 mP
108	5.90	−0.44	18 00 43	−24 04 55	0.45	0.45	in W28A2=G5.9-0.4=G5.899-0.427, in W28=RCW145	IRGr	R = 3.0 LD = 0.4 mP compact
109	6.15	−0.64	18 02 01	−23 57 40	1.6	1.6	in G6.1-0.6=G6.083-0.117, in W28=RCW145	IRGr	R = 2.6 LD = 1.2
110	8.03	0.41	18 02 05	−21 48 12	1.2	0.9	in G8.1+0.2=G8.137+0.228	IRCC	mP
111	8.06	0.43	18 02 06	−21 46 21	1.8	1.2	in G8.1+0.2=G8.137+0.228	IRC	mP
112	10.31	−0.14	18 08 56	−20 05 30	1.4	1.1	in W31	IRCC	R = 6.0 LD = 2.4 mP
113	10.32	−0.15	18 09 00	−20 04 57	1.3	1.2	in W31	IRC	R = 6.0 LD = 2.3 mP
114	12.91	−0.26	18 14 40	−17 52 07	1.2	0.8	in W33C = G12.9-0.3 = G12.909-0.277	IRCC	R = 4.5 LD = 1.6 deeply embedded
115	13.18	0.05	18 14 05	−17 28 40	1.9	1.7	in G13.2+0.0 = G13.186+0.045	IRGr	R = 5.8 LD = 3.2
116	13.88	0.28	18 14 36	−16 45 17	1.2	0.8	in G13.875+0.282	IRC	R_n = 5.6 R_f = 13.8,deeply emb.
117	23.23	−0.24	18 34 27	−9 15 44	1.2	1.0	in G22.8-0.5 = G22.760-0.485	IRCC	R = 12.5 LD = 4.4
118	24.19	0.29	18 34 20	−8 21 27	1.3	1.1	in G23.538-0.041	IRCC	R = 11.6 LD = 4.4
119	23.93	0.28	18 33 54	−8 07 32	1.0	0.7	in G23.7+0.2 = G23.706+0.171	IRCC	
120	25.58	0.99	18 34 25	−7 54 50	0.6	0.5	in G24.0+0.2 = G23.956+0.152	IRGr	R = 12.0 LD = 2.1 compact
121	25.00	0.77	18 34 10	−7 18 01	1.2	1.0	in G24.467+0.489	IRC	R = 9.0 LD = 3.1 deeply emb.
122	26.84	0.65	18 37 58	−6 53 00	2.9	1.9	in G25.253-0.150, in W42	IRC	R = 4.3 LD = 3.8 loose
123	28.82	−0.09	18 44 15	−4 17 55	0.6	0.5	in G28.295-0.377	IRCC	compact,deeply embedded
124	29.86	0.72	18 43 16	−3 35 42	1.2	1.2	in G28.801+0.174	IRCC	R = 9.0 LD = 3.1
125	31.12	0.58	18 46 04	−2 39 19	0.6	0.4	in G29.9-0.0=G29.944-0.042	IRGr	R = 9.0 LD = 1.4 compact
126	33.92	0.11	18 52 51	0 55 28	1.1	1.1	in G33.914+0.111	IRCC	R = 8.3 LD = 2.7
127	34.26	0.15	18 53 20	1 14 39	1.4	1.1	in G34.3+0.1=G34.254+0.144, in W44	IRC	R = 3.7 LD = 1.5 mP
128	34.25	0.13	18 53 22	1 13 58	0.8	0.6	in G34.3+0.1=G34.254+0.144, in W44	IRCC	R = 3.7 LD = 0.9 mP
129	35.20	−0.74	18 58 13	1 40 37	1.3	1.0	in G35.2-0.74 IR Neb., in G35.2-0.74 Molec. Cloud[d]	IRCC	R = 2.3 LD = 1.3
130	35.65	−0.04	18 56 32	2 24 03	2.0	1.7	in G35.663-0.030	IRC	R = 3.5 LD = 2.0 loose
131	42.12	−0.62	19 10 31	7 52 57	1.7	1.3	in G42.108-0.623	IRC	R_n = 5.1 R_f = 9.8
132[e]	43.17	0.03	19 10 11	9 07 03	1.0	0.9	in W49A = G43.2+0.0, in W49	IRGr	R = 13.9 LD = 4.0
133	43.22	−0.05	19 10 33	9 07 37	1.1	1.1	in G43.231-0.054	IRGr	R_n = 0.6 R_f = 13.9
134	45.13	0.14	19 13 27	10 54 27	1.2	1.2	in G45.125+0.136	IRCC	R = 9.7 LD = 3.4 mP
135	45.12	0.13	19 13 28	10 53 35	0.7	0.7	in G45.125+0.136	IRCC	R = 9.7 LD = 2.0 mP compact
136	45.48	0.13	19 14 09	11 12 32	1.3	1.0	in G45.475+0.130	IRCC	R = 9.7 LD = 3.7 deeply embedded
137	45.82	−0.29	19 16 19	11 19 08	1.6	1.4	in G45.8-0.3 = G45.824-0.290	IRCC	
138	48.92	−0.28	19 22 15	14 03 32	1.9	1.6	in G48.9-0.3 = G48.930-0.286, in W51	IRC	R = 7.5 LD = 4.1 mP deeply emb.
139	48.99	−0.30	19 22 26	14 06 54	2.2	2.0	in W51B = G49.0-0.3, in W51	IRC	R = 7.5 LD = 4.8 mP loose
140	49.06	−0.28	19 22 30	14 11 03	2.1	2.1	in G49.1-0.3 = G49.060-0.260, in W51	IRCC	R = 7.5 LD = 4.6
141	49.08	−0.37	19 22 53	14 09 22	1.5	1.3	in G49.1-0.4 = G49.076-0.377, in W51	IRGr	R = 7.5 LD = 3.3 deeply embedded
142	49.38	−0.27	19 23 04	14 28 05	1.0	1.0	in G49.4-0.3 = G49.384-0.298, in W51	IRCC	R = 7.5 LD = 2.2
143	49.39	−0.30	19 23 14	14 27 33	1.4	1.3	in G49.4-0.5 = G49.437-0.465, in W51	IRGr	R = 7.5 LD = 3.1 mP
144	49.42	−0.31	19 23 19	14 29 23	1.3	1.0	in W51	IRCC	R = 7.5 LD = 2.8 mP
145	49.48	−0.33	19 23 29	14 31 43	1.3	1.3	related to W51A = G49.5-0.4 = G49.486-0.381, in W51	IRCC	R = 7.5 LD = 2.8 mP
146	49.49	−0.34	19 23 35	14 32 02	0.9	0.9	related to W51A = G49.5-0.4 = G49.486-0.381, in W51	IRCC	R = 7.5 LD = 2.0 mP
147	49.46	−0.35	19 23 33	14 29 47	0.6	0.6	in W51	IRCC	R = 7.5 LD = 1.3
148	49.46	−0.39	19 23 41	14 29 15	0.6	0.6	in W51A,G49.5-0.4,G49.486-0.381, in W51	IRCC	R = 7.5 LD = 1.3 m5
149	49.48	−0.39	19 23 43	14 29 55	1.5	0.7	in W51A,G49.5-0.4,G49.486-0.381, in W51,[c]	IRCC	R = 7.5 LD = 3.3 m5 deeply emb.
150	49.49	−0.38	19 23 42	14 30 47	0.6	0.3	in W51A,G49.5-0.4,G49.486-0.381, in W51,[b]	IRCC	R = 7.5 LD = 1.3 m5 deeply emb.
151	49.49	−0.38	19 23 43	14 30 34	0.8	0.6	in W51A,G49.5-0.4,G49.486-0.381, in W51,[b]	IRCC	R = 7.5 LD = 1.7 m5 deeply emb.
152	49.49	−0.37	19 23 40	14 31 13	0.7	0.7	in W51A,G49.5-0.4,G49.486-0.381, in W51,[a]	IRCC	R = 7.5 LD = 1.5 m5 deeply emb.
153	49.54	−0.38	19 23 48	14 33 15	1.1	0.9	in W51	IRCC	R = 7.5 LD = 2.4 mP deeply emb.
154	49.54	−0.39	19 23 51	14 32 57	1.0	1.0	in W51	IRCC	R = 7.5 LD = 2.2 mP deeply emb.
155	49.59	−0.39	19 23 55	14 35 40	1.1	1.1	in G49.6-0.4 = G49.582-0.382, in W51	IRC	R = 7.5 LD = 2.4 deeply embedded
156	54.08	−0.07	19 31 43	18 41 57	1.8	1.8	in G54.092-0.066	IRGr	R_n = 3.9 R_f = 7.9
157	51.36	−0.01	19 26 02	16 20 10	2.3	1.7	in G51.362-0.001	IRGr	R_n = 5.0 R_f = 7.5
158	60.88	−0.13	19 46 20	24 35 22	1.1	0.9	in Sh2-87 IR Nebula = G60.888-0.127	IRC	R = 2.7 LD = 0.9 deeply embedded
159	78.88	0.71	20 29 24	40 11 14	0.9	0.8	related to AFGL2591[f]	IRCC	R = 1.0 LD = 0.3 deeply embedded
160[g]	111.56	0.75	23 13 59	61 27 01	1.5	1.1	in NGC 7538-IRS9	IRCC	R = 2.8 LD = 1.2 mT deeply emb.
161	114.63	14.51	22 38 45	75 11 38	1.5	1.0	in LDN1251B IR Nebula, in dark nebula LDN1251	IRGr	R = 0.2 LD = 0.1
162	132.16	−0.73	2 08 05	60 45 53	1.9	1.5	in G132.2-0.7 = G132.157-0.725	IRGr	
163[h]	208.72	−19.20	5 35 27	−5 03 56	1.5	0.9	related to IRAS 05329-0505, in OMC-3	IRGr	R = 0.5 LD = 0.2
164	351.47	−0.46	17 25 32	−36 21 58	0.8	0.8	in G351.467-0.462	IRC	R_n = 4.0 R_f = 15.8
165	351.64	−1.25	17 29 17	−36 40 03	2.0	1.4	in G351.6-1.3 = G351.613-1.270	IRC	R_n = 2.6 R_f = 17.2 deeply emb.
166	351.69	−1.15	17 29 02	−36 33 53	1.8	1.5	in G351.694-1.165	IRC	R = 2.7 LD = 1.4
167	356.30	−0.19	17 37 18	−32 10 48	0.7	0.6	in G356.307-0.210 = IRAS 17341-3208	IRGr	R_n = 1.0 R_f = 19.0

Notes: [a] in W51d = W51-IRS2 (Goldader & Wynn-Wiliams 1994) , [b] in W51e = W51-IRS1-North (Goldader & Wynn-Wiliams 1994), [c] in W51-IRS1-South (Goldader & Wynn-Wiliams 1994), [d] Tapia et al. (1985), [e] quadruplet with W49A, W49A-east and W49A-southwest clusters (Bica et al. 2003), [f] the 2MASS images indicate several stellar sources which suggest a small cluster or stellar group around the massive YSO (Marengo et al. 2000), [g] NGC 7538 IR Cluster in Bica et al. (2003) can be divided into a large loose NW and a compact SE (NGC 7538-IRS1 Cluster) components. These two clusters together with the present object form a triplet, [h] the 2MASS images indicate stellar sources which suggest a small stellar group.

as planetary nebulae. The present results from inspections of J, H and K_s images indicate or confirm (e.g. Acker 1992) that K3-50, Sh2-128, BFS32 = PK149-1.1, IC2120 = PK169-0.1, Sh2-267 = PK196-1.1 and Sh2-271 = PK197-2.1 are not planetary nebulae.

We included in Table 1 new embedded clusters and stellar groups related to optical reflection nebulae. This type of relation has been discussed in Dutra & Bica (2001). These objects appear to be less massive clusters or stellar groups where no ionizing star was formed. The objects in Soares & Bica (2002)

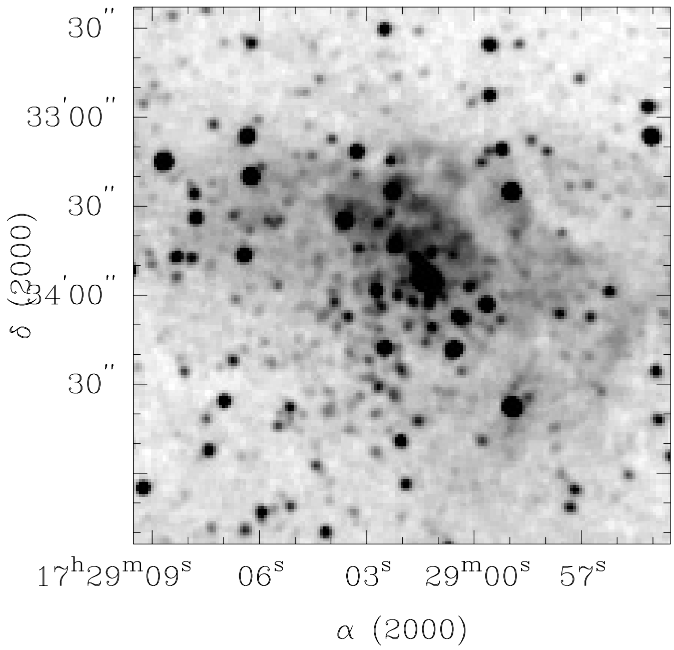

Fig. 3. 3′ × 3′ 2MASS K_s image of Object 166 in the radio nebula G351.694-1.165.

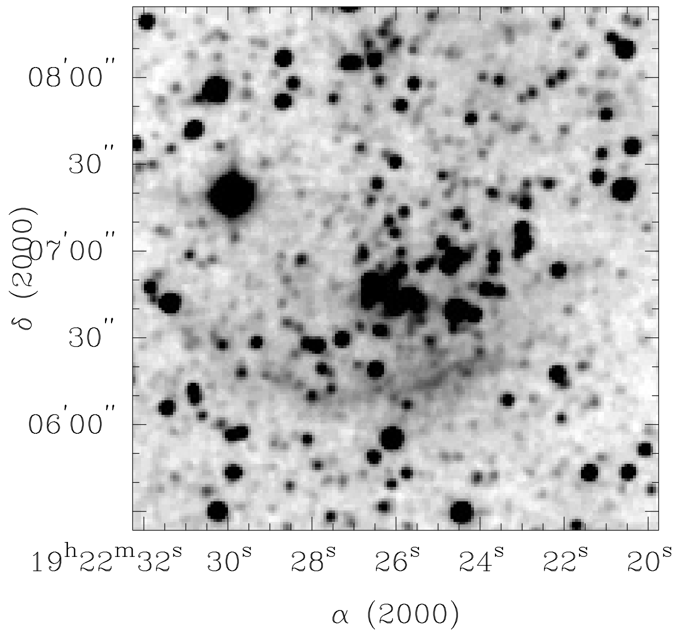

Fig. 4. 3′ × 3′ 2MASS K_s image of Object 139 in the radio nebula W51B = G49.0-0.3.

are of this type or close to its limit towards ionizing stars. The present objects that are related to van den Bergh′s (1966) and van den Bergh & Herbst′s (1975) reflection nebulae are more probably of this type.

4. Discussion

For the present sample (Tables 1 and 2) there occur 42 clusters which are members of pairs, triplets, quadruplets or quintuplet. The quintuplet occurs in W51. That number corresponds to a fraction of 25%, confirming the properties of the two previous samples (Bica et al. 2003 and Paper I). In the present sample multiplicity occurs more often among objects coming from the radio sample, which amount to 24 objects. As discussed in our two previous papers (Bica et al. 2003 and Paper I) multiplicity must play a significant role in the early dynamical evolution of star clusters.

The present results confirm that W51 is a prominent star forming complex in the Milky Way (Goldader & Wynn-Wiliams 1994 and references therein), or that some depth effects occur since this is the eastern tangent point of the Sagittarius-Carina Arm. Table 2 shows that 18 objects are related to W51: 3 IRCs, 2 IRGrs and 13 IRCCs.

Figure 5 shows the angular distributions of the present samples (Tables 1 and 2). Objects from the radio sample are mainly located between $350° < \ell < 360°$ and $0° < \ell < 60°$ corresponding to internal arms and where absorption in the Galaxy shows a pronounced increase (Dutra & Bica 2000b). Objects coming from the optical sample are more evenly distributed across the surveyed region, including directions of the Local, Perseus and Outer Arms. Both samples have objects in directions of the Sagittarius-Carina Arm, but more probably objects related to optical nebulae belong to it.

Figure 6 shows the distance histograms for the objects (Tables 1 and 2). In cases of distance ambiguity we assumed their near distance as a lower limit for the histogram analysis. The optical sample has a pronounced peak at 2 kpc, but has important contributions up to 4 kpc. The histogram of the radio sample covers a wide distance range. The pronounced peak at 7.5 kpc corresponds to the large number of objects in the W51 complex. A secondary peak occurs for ≈9 kpc. Radio objects are also significantly distributed in the range 2–4 kpc.

Figure 7 shows the linear size histograms for the objects (Tables 1 and 2). Objects with distance ambiguity were excluded. The histogram of objects coming from the optical nebulae sample is remarkably similar to that obtained in Bica et al. (2003) and its counterpart of Paper I, skewed with a peak at about 1 pc. The histogram of objects from the radio nebulae sample is more evenly distributed, with a peak at about 2 pc, likewise its counterpart in Paper I.

Concerning SNRs, one probable IRGr is in the area of the radio SNR GG5.2-2.6, and one in that of G5.321-0.974 (Table 2), confirming that such relations are a rare phenomenon (Paper I).

4.1. Total sample of known objects

Considering the results of the present work, Paper I and the literature objects indicated in Sect. 1, the total sample of known infrared clusters, stellar groups and candidates is now 661.

Figure 8 shows the angular distribution in galactic coordinates of the total sample. Now the whole Milky Way has been more uniformly surveyed, which was not the case of the literature sample (see Fig. 1 of Bica et al. 2003). The objects towards the central parts are distributed more closely to the plane, suggesting larger distances on the average. The objects

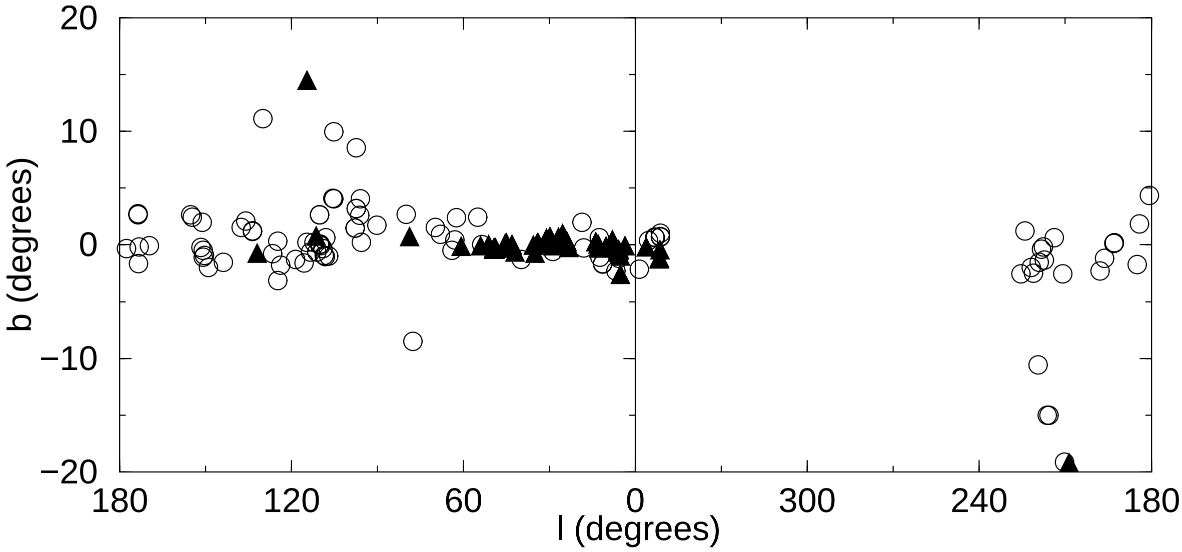

Fig. 5. Angular distribution of infrared clusters coming from optical (Table 1) represented by open circles, and radio nebulae (Table 2) represented by filled triangles.

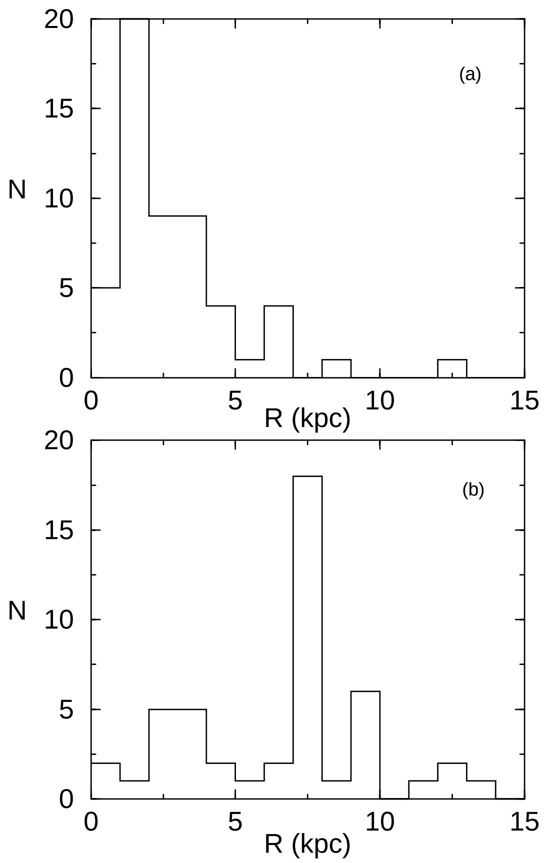

Fig. 6. Distance histograms for the samples coming from: panel **a)** optical (Table 1) and panel **b)** radio nebulae (Table 2).

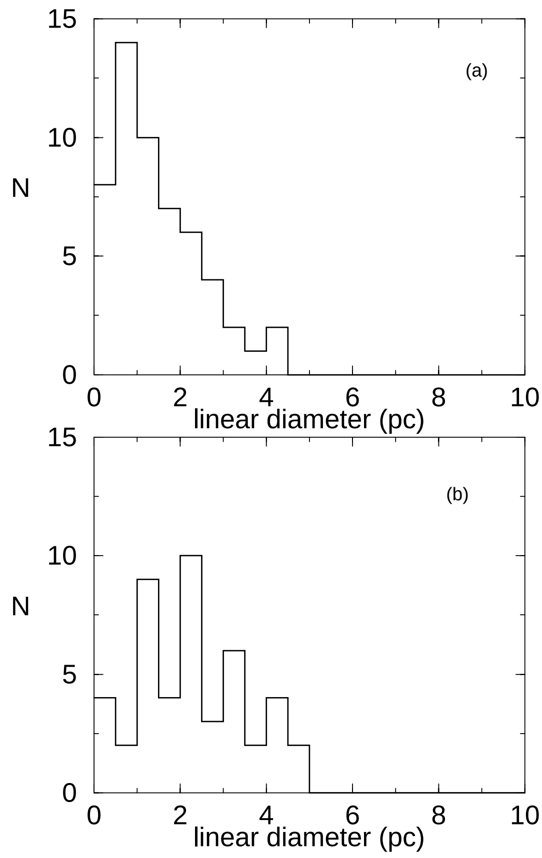

Fig. 7. Linear major dimension histograms for the samples coming from: panel **a)** optical (Table 1) and panel **b)** radio nebulae (Table 2).

at higher latitudes around the anticentre are in the nearby Orion and Taurus complexes.

Figure 9 shows the distance histogram for the total sample. The distribution peak occurs at 1.5 kpc, showing that a typical IR cluster or stellar group is a relatively close object. Most of the objects are in the range 1–4 kpc, but an important sample also occurs for 5–9 kpc. A few objects exceed 10 kpc.

Figure 10 shows the linear size histogram for the total sample. The enormous sample that we are dealing with shows that embedded clusters are typically small, less than 2 parsecs in size, and hardly exceeding 4 pc. This must reflect the dimensions of the regions in molecular clouds where star formation is efficient enough to create zones of high stellar densities.

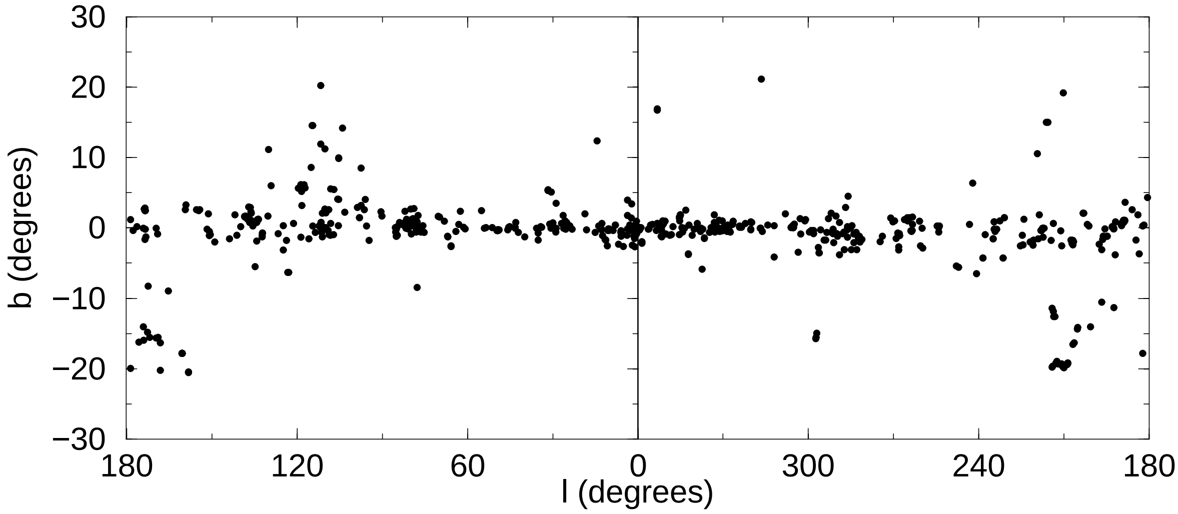

Fig. 8. Angular distribution of infrared clusters of all known IR clusters, stellar groups and candidates.

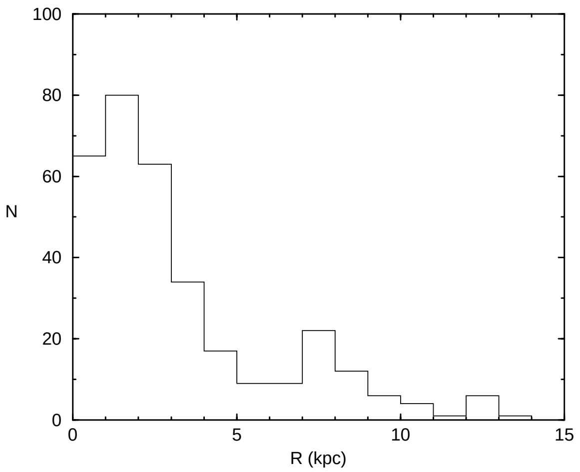

Fig. 9. Distance histogram for all known IR clusters, stellar groups and candidates.

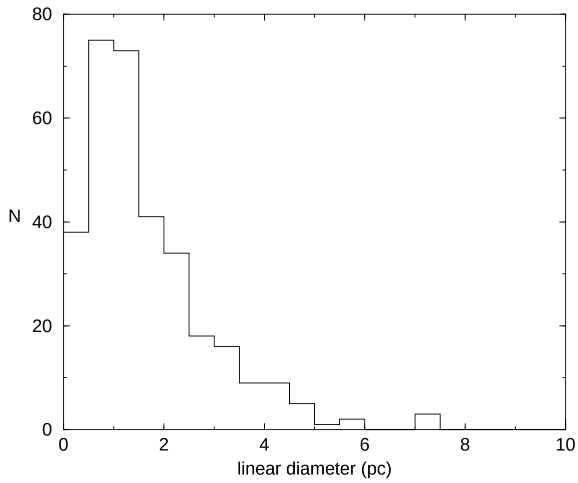

Fig. 10. Linear major dimension histogram for all known IR clusters, stellar groups and candidates.

The present results suggest that the extent of such regions does not vary much from cloud to cloud.

We can also estimate the density increase of objects along the Galactic disk by comparing the samples in Bica et al. (2003) and the present total sample. Considering clusters with $|b| < 5°$ the former sample provided 0.53 objects (degree)$^{-1}$ along Galactic longitude, while the present overall sample yields 1.57 (degree)$^{-1}$.

The angular distributions and distances indicate that the now known overall sample of embedded clusters and stellar groups arises mostly in external arms, in the near side of internal arms and to a certain extent central parts of the Galaxy. Beyond these regions, especially towards the inner Galaxy, line-of-sight absorption effects must be too strong, even for the near IR domain.

4.1.1. Sensitivity of surveys

It is interesting to compare the spatial distribution of infrared clusters and stellar groups with those of the optical and radio nebulae. A decrease of clusters with distance would favour distance/reddening effects on detectability while other distributions might suggest that many nebulae do not harbour any cluster. We study the available objects in the whole plane, including the present sample, that of Paper I and the previously catalogued clusters (Bica et al. 2003). Distance information is available for 958 optical and 358 radio nebulae. There are 232 clusters or groups related to optical nebulae and 119 to radio nebulae with distance estimates. The comparison is made in Fig. 11. The blowup for optical objects (upper right panel) suggests a detection decrease with distance for $d > 2.5$ kpc. For the radio sample the distance decrease is clear for $d > 5$ kpc (lower left panel). These results suggest that nebulae with distance information in general harbour a cluster or stellar group and that many remain undetected owing to a reddening/distance horizon effect. However, the total number of nebulae in the catalogues is much larger (Sect. 3) than those with velocity (distance) information, which suggests that many deal with structural details of the nebular complexes, which do not necessarily harbour any cluster.

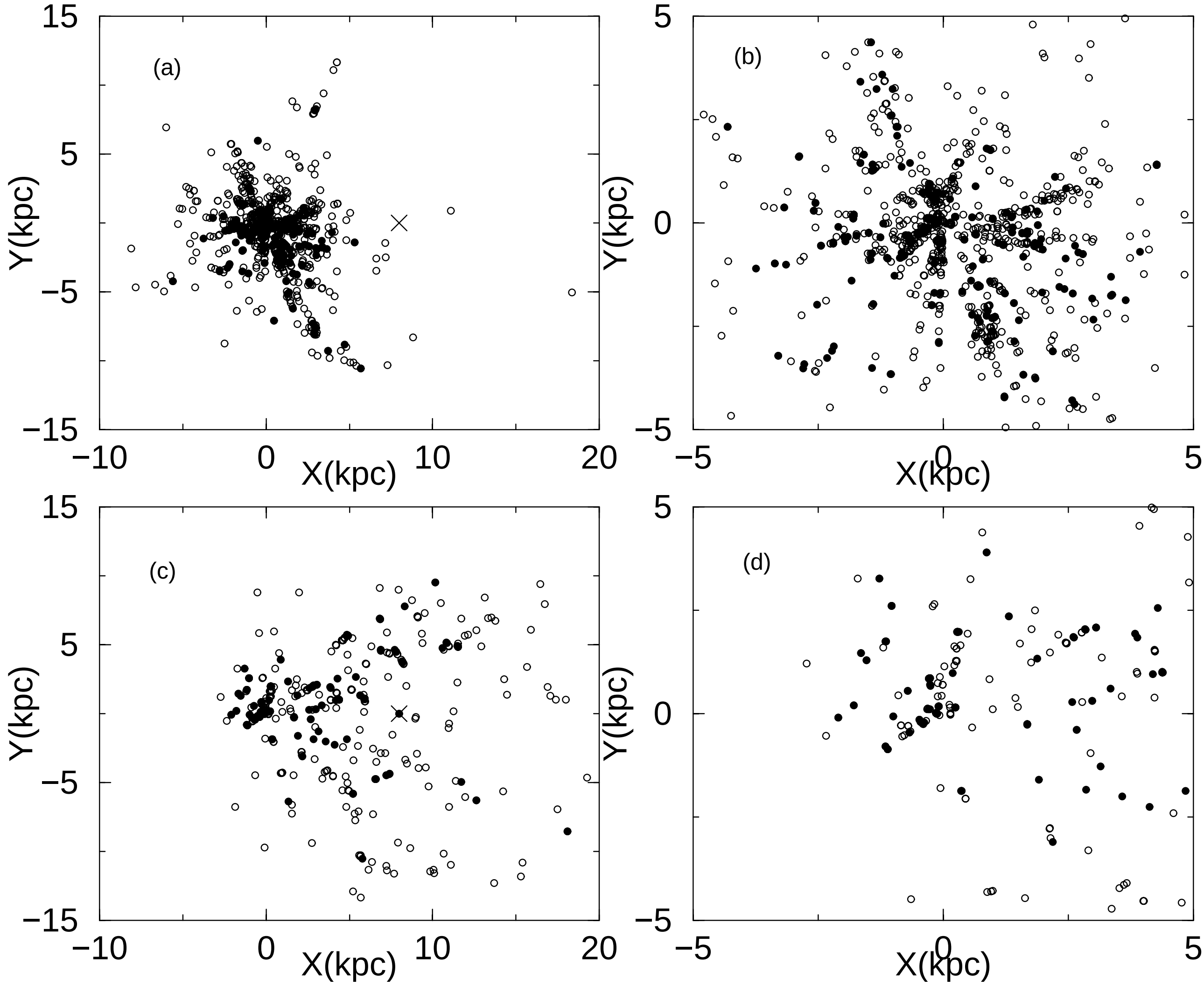

Fig. 11. Projection on the Galactic plane (heliocentric coordinates) of embedded clusters and nebulae. Upper left and lower left panels correspond to optical and radio nebulae, respectively. Upper right and lower right panels are the respective blowups. Open circles are nebulae, filled circles are clusters. Cross indicates the Galactic centre.

5. Concluding remarks

We searched for embedded star clusters and stellar groups in the directions of 1361 optical and 826 radio nebulae in the Equatorial and Northern Milky Way (in the region $350^\circ < \ell < 360^\circ$, $0^\circ < \ell < 230^\circ$) using J, H and K_s images from the 2MASS all-sky release Atlas. A total of 167 new infrared clusters, stellar groups and candidates were found. Together with 179 discoveries from Paper I, the present method provided a total of 346 new objects. This number is larger than that of all previously known infrared clusters, stellar groups and candidates in the literature, which amount to 315 objects.

The physical properties of the present sample are similar to those of its southern counterpart (Paper I), in particular concerning the size distribution of clusters coming from the optical and radio nebulae samples. Multiplicity appears to affect about 25% of the embedded clusters, suggesting that interactions and mergers can affect their early dynamical evolution. Objects from the optical nebulae sample are on the average closer (at 2–4 kpc) than those from the radio nebulae sample.

The present contribution and that of Paper I provide a fundamental new sample for detailed future studies. Resolved brighter objects may be studied with 2MASS photometry itself, but most of the sample requires large telescopes for deep photometry.

Considering the results of the present work, Paper I and the literature objects indicated in Sect. 1, the total sample of known infrared clusters, stellar groups and candidates now amounts to 661 objects. Most are located nearby (1–4 kpc) and they are typically smaller than 2 pc.

Much work is yet to be done with 2MASS, especially in the search of more evolved disk clusters away from nebulae. Systematic visual searches in specific areas and searches using automated methods will certainly provide many new discoveries.

Acknowledgements. This publication makes use of data products from the Two Micron All Sky Survey, which is a joint project of the University of Massachusetts and the Infrared Processing and Analysis Center/California Institute of Technology, funded by the National Aeronautics and Space Administration and the National Science

Foundation. We employed data from CDS/Simbad (Strasbourg). We thank the referee Dr. F. Comerón for interesting remarks. We acknowledge support from the Brazilian Institutions CNPq and FAPESP. CMD acknowledges FAPESP for a post-doc fellowship (Proc. 00/11864-6).

References

Acker, A., Ochsenbein, F., Stenholm, B., et al. 1992, Strasbourg-ESO Catalogue of Galactic Planetary Nebulae, CDS, Strasbourg
Alter, G., Ruprecht, J., & Vanysek, V. 1970, Catalogue of star clusters and associations + supplements, 2nd ed. (Budapest: Akad. Kiado)
Bernes, C. 1977, A&A, 29, 65
Bica, E., Dutra, C., & Barbuy, B. 2003, A&A, 397, 177
Blitz, L., Fich, M., & Stark, A. A. 1982, ApJS, 49, 183
Carpenter, J. M. 2000, AJ, 120, 3139
Cederblad, S. 1946, MeLu2, 119, 1
Cohen, M. 1980, AJ, 85, 29
Deharveng, L., Zavagno, A., Cruz-González, I., et al. 1997, A&A, 317, 459
Deharveng, L., Zavagno, A., Salas, L., et al. 2003, A&A, 399, 1135
Dias, W. S., Alessi, B. S., Moitinho, A., & Lépine, J. R. D. 2002, A&A, 389, 871
Downes, D., Wilson, T. L., Bieging, J., & Wink, J. 1980, A&AS, 40, 379
Dutra, C. M., & Bica, E. 2000a, A&A, 359, L9
Dutra, C. M., & Bica, E. 2000b, A&A, 359, 347
Dutra, C. M., & Bica, E. 2001, A&A, 376, 434
Dutra, C. M., & Bica, E. 2002, A&A, 383, 631
Dutra, C. M., Bica, E., Soares, J. B., & Barbuy, B. 2003a, A&A, 400, 533
Dutra, C. M., Ortolani, S., Bica, E., et al. 2003b, A&A, submitted
Georgelin, Y. M., Georgelin, Y. P., & Roux, S. 1973, A&A, 25, 337
Goldader, J. D., & Wynn-Wiliams, C. G. 1994, ApJ, 433, 164
Green, D. A. 2001, in Catalogue of galactic supernova remnants, Muller radio astronomy (Cambridge, UK)
Gyulbudaghian, A. L., Glushkov, Iu. I., & Denisiuk, A. E. 1978, ApJ, 224, L137
Gyulbudaghian, A. L., & Maghakian, T. Y. 1977a, PAZh, 3, 113
Gyulbudaghian, A. L., & Maghakian, T. Y. 1977b, DoSSR, 64, 104
Gyulbudaghian, A. L., & Maghakian, T. Y. 1977c, ATsir, 1, 2
Gyulbudaghian, A. L. 1982a, PAZh, 8, 232
Gyulbudaghian, A. L. 1982b, PAZh, 8, 222
Gyulbudaghian, A. L. 1984a, Afz, 20, 631
Gyulbudaghian, A. L. 1984b, ATsir, 1342, 7
Gum, C. S. 1955, MmRAS, 67, 155
Hodapp, K.-W. 1994, ApJS, 94, 615
Kuchar, T. A., & Clark, F. O. 1997, ApJ, 488, 224
Ivanov, V. D., Borissova, J., Pessev, P., Ivanov, G. R., & Kurtev, R. 2002, A&A, 394, L1
Lada, C. J., & Lada, E. A. 1991, in The formation and evolution of star clusters, 3
Lauberts, A. 1982, ESO/Uppsala survey of the ESO(B) atlas (Garching: ESO)
Lockman, F. J. 1989, ApJS, 71, 469
Lyngå, G. 1987, Computer based catalogue of open cluster data, 5th ed. (Strasbourg: CDS)
Le Duigou, J.-M., & Knödlseder, J. 2002, A&A, 392, 869
Marengo, M., Jayawardhana, R., Fazio, G. G., et al. 2000, ApJ, 541, L63
Neckel, T., & Staude, H. J. 1984, A&A, 131, 200
Parsamian, E. S. 1965, IzArmyan, 18, 146
Parsamian, E. S., & Petrosian, V. M. 1979, SoByu, 51, 3
Reifenstein III, E. C., Wilson, T. L., Burke, B. F., Mezger, P. G., & Altenhoff, W. J. 1970, A&A, 4, 357
Reylé, C., & Robin, A. C. 2002, A&A, 384, 403
Rodgers, A. W., Campbell, C. T., & Whiteoak, J. B. 1960, MNRAS, 121, 103
Soares, J. B., & Bica, E. 2002, A&A, 388, 172
Sharpless, S. 1953, ApJ, 118, 362
Sharpless, S. 1959, ApJS, 4, 257
Skrutskie, M., Schneider, S. E., Stiening, R., et al. 1997, in The Impact of Large Scale Near-IR Sky Surveys, ed. F. Garzon, N. Epchtein, A. Omont, W. B. Burton, & P. Persi (Netherlands: Kluwer), 210, 187
Sugitani, K., Fukui, Y., & Ogura, K. 1991, ApJS, 77, 59
Tapia, M., Roth, M., Persi, P., & Ferrari-Toniolo, M. 1985, MNRAS, 213, 833
van den Bergh, S., & Herbst, W. 1975, AJ, 80, 208
van den Bergh, S. 1966, AJ, 71, 990
van den Bergh, S. 1978, ApJS, 38, 119
von Dorschner, J., & Gurtler, J. 1963, AN, 287, 257
Westerhout, G. 1958, BAN, 14, 215
Wilson, R. W., & Bolton, J. G. 1960, PASP, 72, 331
Wilson, R. M. 1963, AJ, 68, 181
Woodward, C. E., Pipher, J. L., Helfer, H. L., & Forrest, W. J. 1990, ApJ, 365, 252